Stress-modified structural and electronic properties of epitaxial MnAs layers on GaAs

Y. Takagaki, C. Herrmann, J. Herfort, C. Hucho, and K.-J. Friedland
Paul-Drude-Institut für Festkörperelektronik, Hausvogteiplatz 5-7, 10117 Berlin, Germany
(Received 7 October 2008; revised manuscript received 28 November 2008; published 30 December 2008)

We compare the transport properties in MnAs layers epitaxially grown on GaAs substrates with various orientation relationships, including MnAs($1\bar{1}00$)/GaAs(001), MnAs(0001)/GaAs(111), and MnAs($1\bar{1}00$)/GaAs(111). Due to the anisotropic abrupt change in the lattice constants at the phase transition between α- and β-MnAs, the phase-transition stress varies over a wide range depending on the c-axis orientation of MnAs. We employ the temperature range of the phase coexistence to evaluate the strength of the stress. The complex Fermi surface of MnAs is found to alter the Hall coefficient remarkably between holelike and electronlike behaviors in spite of rather subtle changes in the band structure by the strain. We also show that enormously strong pinning of domain walls arises in MnAs layers on GaAs(111)B when in-plane and out-of-plane c-axis orientations are simultaneously present.

DOI: 10.1103/PhysRevB.78.235207 PACS number(s): 75.47.−m, 64.70.K−, 68.35.−p, 72.15.Eb

I. INTRODUCTION

Despite the numerous efforts over half a century, the magnetic properties of MnAs have not been fully understood, as highlighted by the controversy whether the β phase, which occurs for temperatures above the Curie temperature $T_C \approx 40$ °C, is paramagnetic or antiferromagnetic.[1–5] The last decade has witnessed a revival of interest on MnAs motivated by the progress of heteroepitaxy for applications in spintronics. The hybrids of a ferromagnet and a semiconductor are a crucial element in spintronics to perform, for instance, spin injection and detection. MnAs is one of the prospective candidates to fulfill the ferromagnetic part as its Curie temperature is above room temperature and epitaxial growth on GaAs, which is the most widely used semiconductor for spin manipulation, is possible.[6,7] The matchless material purity that molecular-beam epitaxy (MBE) can provide is attractive to settle the unsolved issues on the magnetic properties of MnAs. However, the material properties that epitaxial layers exhibit may differ from the bulk properties due to the strain imposed by the substrates. For instance, the magnetotransport properties of MnAs layers have revealed that even the type of majority carriers depends on the epitaxial orientation relationship.[8,9]

The markedly large influence of the stress originates from two characteristics. (i) The thermal expansion of MnAs is about 1 order of magnitude larger than that of GaAs. (ii) The lattice constant changes abruptly at T_C. At the phase transition between the ferromagnetic α phase and the β phase, the a-axis lattice constant changes discontinuously by a few percent. While the thermal-expansion mismatch leads to tensile stress in epitaxial layers, the stress in the a-axis direction of α-MnAs is, as a consequence, compressive. The discontinuous lattice-constant change does not occur in the c-axis direction. This anisotropy leads to a strong dependence of the nature and the strength of the stress on the epitaxial orientation. In exploring the material properties of MnAs using epitaxial layers, therefore, one needs to be aware of the influences of the stress. On the other hand, stress manipulation through controlling the epitaxial orientation relationship may allow us, for instance, to raise T_C beyond the bulk value.[10]

In this paper, we investigate the transport properties in MnAs layers grown on GaAs substrates with various epitaxial orientation relationships. The specimen includes previously uninvestigated MnAs($1\bar{1}00$)/GaAs(111)B system, which has been made possible by a recently discovered growth procedure. Our attention is mainly focused on two aspects of the transport properties that manifest the stress-induced alteration of structural and electronic properties: (i) the temperature dependence of the resistivity at the phase-transition region around room temperature and (ii) the Hall resistivity at a cryogenic temperature. In addition, we also investigate a phenomenon of strong domain-wall pinning in MnAs layers on GaAs(111)B.

II. SAMPLES

MnAs layers were grown on GaAs substrates in a solid-source MBE chamber. We employ heterostructures having the orientation relationships summarized in Table I. Our main objective is to compare the transport properties in three systems illustrated in Fig. 1: (a) MnAs($1\bar{1}00$)/GaAs(001), (b) MnAs(0001)/GaAs(111)B, and (c) MnAs($1\bar{1}00$)/GaAs(111)B. Widely varied stress environment is realized in these layers due to the distinct c-axis alignment. While the rest of the MnAs layers grown for other substrate orientations in Table I were additionally examined, the stress in these systems is expected to be similar to that in the MnAs($1\bar{1}00$)/GaAs(001) or MnAs($1\bar{1}00$)/GaAs(111)B system due to the common in-plane c-axis alignment.

The MnAs($1\bar{1}00$) layers on GaAs(001) and the MnAs(0001) layers on GaAs(111)B were prepared by conventional MBE growths at substrate temperatures T_s listed in Table I. In the former case, the [0001] and [$11\bar{2}0$] directions of MnAs are parallel to the [$1\bar{1}0$] and [110] directions of GaAs, respectively. (The so-called type-A orientation.[6]) In the latter case, the [$1\bar{1}00$] and [$11\bar{2}0$] directions of MnAs are parallel to the [$11\bar{2}$] and [$1\bar{1}0$] directions of GaAs, respectively. The unconventionally orientated MnAs($1\bar{1}00$) layers

TABLE I. Orientation of GaAs substrates, primary orientation of MnAs layers, growth temperature T_s, layer thickness, temperature interval ΔT for the coexistence of the α and β phases, temperature shift δT for the thermal hysteresis associated with the phase transition between the α and β phases, and transition temperature $T_{\beta\text{-}\gamma}$ between the β and γ phases. For the layers grown by means of solid-phase epitaxy, two values are given for T_s: the deposition temperature of the amorphous layer and the growth temperature for the subsequent conventional growth. The details of the epitaxial orientation can be found in Ref. 12.

Sample No.	Substrate	Orientation	T_s (°C)	Thickness (nm)	ΔT (K)	δT (K)	$T_{\beta\text{-}\gamma}$ (K)
1	(001)	$(1\bar{1}00)$	230	50	29	0.8	371
2	(001)	$\sim(1\bar{1}01)$	180, 250	20	33	2	
3	(001)	$\sim(1\bar{1}00)$	200, 250	130	19	1.7	373
4	(113)A		180, 250	20	33	1.3	
5	(113)A	$\sim(2\bar{3}11)$	200, 250	150	16	0.9	381
6	(113)B	$(1\bar{1}01)$	200, 250	100	30	1.5	
7	(112)B	$(1\bar{1}0l)$	200, 250	145	45	1.5	
8	(111)B	(0001)	250	50	160		395
9	(111)B	(0001)	270	50			
10	(111)B	$\sim(1\bar{1}00)$	220	50			
11	(111)B	$(1\bar{1}00)$	200, 270	50	18	0.6	
12	(331)B	$(1\bar{1}00)$, $(11\bar{2}2)$	200, 250	125	41		420
13	(110)	$(1\bar{1}00)$	200, 250	140	60	3	

on GaAs(111)B were obtained using a growth procedure based on solid-phase epitaxy (SPE).[11] Here, an amorphous MnAs layer with the nominal thickness of 2 nm was deposited at T_s=200 °C. The layer was then crystallized by increasing T_s to 270 °C and closing the shutter for As cell to enhance the surface migration. This procedure leads to a $(1\bar{1}00)$-oriented growth template.[12] The thickness of the *M*-plane MnAs layer was then increased by an additional conventional growth at T_s=270 °C. Due to the threefold symmetry of the substrate, the layers are inevitably composed of structural domains, in which the *c* axis of MnAs is aligned along one of the $\{11\bar{2}\}$ directions of the substrate,[11]

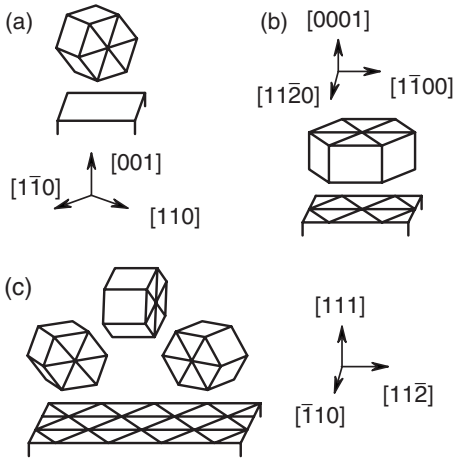

FIG. 1. Schematic view of the epitaxial orientation relationship for (a) MnAs$(1\bar{1}00)$/GaAs(001), (b) MnAs(0001)/GaAs(111), and (c) MnAs$(1\bar{1}00)$/GaAs(111) systems.

as illustrated in Fig. 1(c). The establishment of the epitaxial orientation relationship by means of SPE is overwhelmingly dominated by the bulk strain energy, and so the growth is far less flexible in terms of the lattice mismatch in comparison to the conventional growth.[12] The layers contain a large number of different crystal orientations when the lattice mismatch is large, whereas orientational spread is suppressed if the mismatch is small.

Figure 2(a) shows the atomic-force microscopy (AFM) image of a 50-nm-thick $(1\bar{1}00)$-oriented layer on GaAs(111)B, No. 11. Few-hundred-nanometer large elongated features are found with a mean height modulation of 1.8 nm. The direction of the elongation is parallel to the $\{\bar{1}10\}$ direction; and so, if these features correspond to the structural domains, the magnetic easy axis is oriented in the

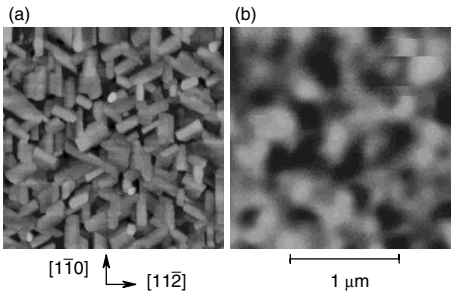

FIG. 2. (a) Atomic- and (b) magnetic-force micrographs of the surface of a MnAs$(1\bar{1}00)$ layer on GaAs(111)B, No. 11. The mean height modulation in (a) is 1.8 nm. The magnetic imaging in (b) was carried out for a demagnetized state at room temperature. The contrast shows the strength of the normal component of magnetic field.

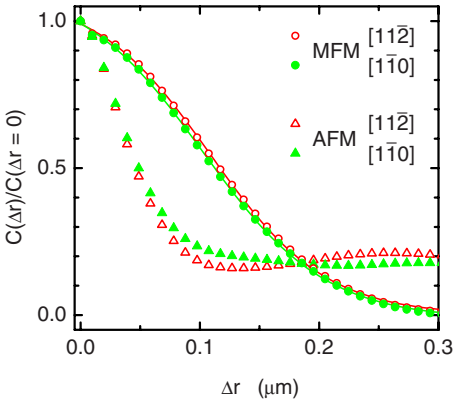

FIG. 3. (Color online) Autocorrelation $C(\Delta\mathbf{r})$ of AFM and MFM images obtained from an area of 5×5 μm^2 of a MnAs$(1\bar{1}00)$ layer on GaAs(111)B, No. 11. The displacement $\Delta\mathbf{r}$ is taken along the $[11\bar{2}]$ and $[1\bar{1}0]$ directions of the substrate for the open and filled symbols, respectively. The curves show fits to a form $c_1+c_2/\{1+\exp[(\Delta r-c_3)/c_4]\}$ with c_i being fit parameters.

direction of the elongation. (We thus do not need to pay attention to the possibility of inclination of magnetization by shape anisotropy.) In Fig. 2(b), we show a magnetic-force microscopy (MFM) image of the surface shown in Fig. 2(a) in a demagnetized state. As we show in Sec. III, the MnAs layer is almost completely in the ferromagnetic α phase at the temperature (room temperature) the image was taken. In Fig. 3, we plot the autocorrelation

$$C(\Delta\mathbf{r}) = \langle h(\mathbf{r})h(\mathbf{r}+\Delta\mathbf{r})\rangle_{\mathbf{r}} \tag{1}$$

when $\Delta\mathbf{r}$ is set to be along the $[11\bar{2}]$ and $[1\bar{1}0]$ directions of the substrate. Here, $h(\mathbf{r})$ is the deviation from the mean "height" at position $\mathbf{r}$. The average $\langle\cdots\rangle$ is taken over $\mathbf{r}$. The autocorrelation of the MFM image, shown by circles, decays by a factor of 2.4 slower than that of the AFM image, shown by triangles. From the decay of the correlation $C(\Delta\mathbf{r})=\frac{1}{2}C(0)$, the size of the magnetic domains is estimated to be $0.11-0.12$ μm. Although the crystalline anisotropy should give rise to a maximal difference between the GaAs$[11\bar{2}]$ and GaAs$[1\bar{1}0]$ directions, the autocorrelation of the AFM image in the two directions is almost identical, in spite of the unambiguous anisotropy seen in Fig. 2(a). Autocorrelation is thus suggested to be unsuitable for providing information regarding anisotropy. We have not been able to examine so far whether the threefold symmetry is reflected in the MFM image.

As demonstrated in Ref. 11 by the magnetic hysteresis of magnetization measured using superconducting-quantum-interference-device (SQUID) magnetometer, the three magnetization components associated with the structural domains are practically independent of each other. This suggests that the structural domains are large enough to sustain unperturbed magnetic domains. That the magnetic domain size in Fig. 2(b) is comparable to the value typically found in MnAs layers having a single in-plane orientation, i.e., $(1\bar{1}00)$-oriented MnAs layers on GaAs(001), supports this interpretation. Nevertheless, the difference in the correlation length between the MFM and AFM images may evidence magnetic synchronization of small structural domains with a neighboring large structural domain. In this respect, we call our attention to the flipping of local magnetic moments during the probe scan seen in the upper-right area of Fig. 2(b). Such flips do not occur in $(1\bar{1}00)$-oriented MnAs layers on GaAs(001) due to the strong uniaxial magnetocrystalline anisotropy. The effective weakening of the uniaxial anisotropy may be a consequence of magnetic interaction among the magnetic moments inclined by 60° with each other. The local magnetic coupling maintains the amount of magnetization along each of the easy axes, on average, to be one third of the total magnetization and leaves the three magnetization components to be independent of each other.

As we present in Secs. III and IV, we measured the resistance of these MnAs layers using lock-in technique. The measurements at a cryogenic temperature were carried out using Hall-bar devices. The patterning of the epitaxial layers into a Hall-bar geometry was performed by means of lithography and Ar-ion milling. For measurements around room temperature, van der Pauw devices were also employed. The excitation current I for the measurements was about 1 μA around room temperature and about 10 μA when the temperature was at $T=0.3$ K.

III. PHASE TRANSITIONS

A. Coexistence of the α and β phases

The coexistence of the α and β phases of MnAs in epitaxial layers is a consequence of the minimization of elastic energy through stress cancelation.[13] The critical thickness for coherent growth of MnAs on GaAs is less than 1 nm,[14,15] and so epitaxial layers are almost fully relaxed at the growth temperature. While cooling the layers to room temperature following the growth, they are tensile stressed as the thermal-expansion coefficient of MnAs is significantly large. MnAs undergoes a phase transition from the γ phase, which is the phase during the MnAs growth, to the β phase at a temperature of about 400 K, where the crystal structure changes from hexagonal to orthorhombic. As far as the stress is concerned, however, this phase transition has no significance.

The stress is dramatically altered at the simultaneous magnetic and structural phase transitions between the α and β phases at T_C. This is because the phase transition involves a discontinuous lattice-constant change of 1.2% in the a-axis direction. Let us now consider a specific case of a MnAs$(1\bar{1}00)$ layer on GaAs(001). The MnAs layers are suddenly compressively stressed in the a-axis direction in α-MnAs while the layers are still tensile stressed in the c-axis direction. The strain energy can be lowered by retaining both of the phases in the a-axis direction to compensate the tensile and compressive stresses. The MnAs layers hence develop a stripe pattern of alternating α and β phases in the MnAs$[11\bar{2}0]$ direction. The temperature range of the phase coexistence sensitively reflects the stress that the layers are subjected to. We emphasize that the stress in MnAs layers is so strong that the layers crack when the thickness exceeds

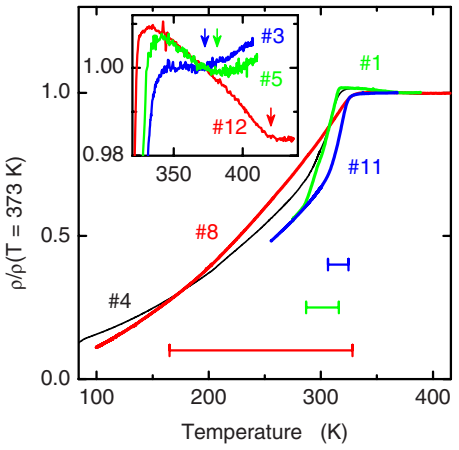

FIG. 4. (Color online) Temperature dependence of resistivity ρ normalized to the value at temperature $T=373$ K. The green and red curves correspond, respectively, to an M-plane MnAs layer on GaAs(001), No. 1, and a C-plane MnAs layer on GaAs(111)B, No. 8, grown by conventional MBE. The blue curve shows ρ in an M-plane MnAs layer grown on GaAs(111)B by means of SPE, No. 11. For the thin black curve, the MnAs layer was grown on GaAs(113)A by means of SPE, No. 4. The temperature interval for the coexistence of the α and β phases is indicated by the horizontal bars. The blue, green, and red curves in the inset correspond to MnAs layers on (001)-, No. 3, (113)A-, No. 5, and (331)B-, No. 12, oriented substrates grown by means of SPE, respectively. The arrows indicate the phase-transition temperature $T_{\beta\text{-}\gamma}$ between the β and γ phases.

about 0.5 μm. Stress, therefore, has a profound impact on the material properties of MnAs layers.

In Fig. 4, we show the temperature dependence of the resistivity ρ normalized to the value at 373 K. At the first-order phase transition at T_C, the resistivity changes discontinuously between the α and β phases ($\rho_\beta/\rho_\alpha \approx 1.4$). The temperature dependence of ρ in the phase coexistence regime, which is indicated by the horizontal bars in Fig. 4, is nearly linear and is determined mainly by the change in the phase fractions. For temperatures lower than the coexistence regime, the temperature dependence of ρ is attributed to the phonon and magnon scatterings. The temperature coefficient for β-MnAs is intriguingly negative.[16] The negative temperature dependence was discussed in Ref. 5 as a possible indication of an antiferromagnetic order in β-MnAs.[3,4] Several other mechanisms have also been proposed to explain the anomaly around T_C.[17]

The green curve in Fig. 4 corresponds to a MnAs($1\bar{1}00$) layer on GaAs(001), No. 1, for which there exits a large literature.[7] The phase coexistence occurs over a temperature width of about 30 K. In comparison, the temperature interval in the MnAs(0001)/GaAs(111)B system, No. 8, red curve, is by a factor of $\sim$5 wider. The phase-transition stress is thus indicated to be stronger in the C-plane layers than in the M-plane layers. For C-plane MnAs layers, the abrupt lattice-constant change occurs in both of the in-plane orthogonal directions, giving rise to the strong phase-transition stress. Instead of the stripe pattern in M-plane layers, the phase coexistence in C-plane layers takes place in the form of islands of β-MnAs embedded in a honeycomb network of α-MnAs.[18]

The temperature interval ΔT is related to the strain $\eta(=0.01)$ as[13]

$$\Delta T_{\parallel} = \frac{E_a \eta^2 T_C}{(1-\nu^2)L} \tag{2}$$

when the c axis of MnAs lies in the surface plane. Here, L is the latent heat and ν is the Poisson ratio. We have taken into account the anisotropy of the Young modulus E. The orientational dependence of E on a hexagonal crystal is described by the expression

$$E^{-1} = s_{11}\sin^4\theta + s_{33}\cos^4\theta + (s_{44}+2s_{13})\sin^2\theta\cos^2\theta, \tag{3}$$

where θ is the angle between the direction of stress and the c axis. Using the value of the elastic compliance constants s_{ij} in Ref. 19, the Young modulus in the a-axis direction ($E_a = 38$ GPa) is estimated to be about one third of that in the c-axis direction ($E_c = 110$ GPa). When the c axis is normal to the surface, ΔT is given by

$$\Delta T_{\perp} = \frac{2E_a \eta^2 T_C}{(1-\nu)L}. \tag{4}$$

The theory thus predicts ΔT for the C-plane layers to be larger by a factor of $2(1+\nu)$ than that for the M-plane layers. The factor of 2 presumably reflects the dimensionality of the phase coexistence: the layers are stressed in two directions in Eq. (4) and in one direction in Eq. (2). The contributions from the two orthogonal directions are merely added as Eqs. (2) and (4) are the lowest-order evaluation. The experimentally observed difference in ΔT between the M and C planes is considerably larger than this prediction. Given that Eq. (2) provides a reasonable estimate for ΔT in M-plane layers,[13] the disagreement suggests that higher-order terms can no longer be ignored for the C-plane layers as, among others, ΔT is not small in comparison to T_C. (The large anisotropy of E does not play a role as ΔT is related only to the Young modulus in the direction of the phase-transition stress.)

Contrary to the enhancement of the phase coexistence in C-plane MnAs layers, ΔT in M-plane layers becomes small when the substrate is GaAs(111)B instead of GaAs(001). That is, the layers in the MnAs($1\bar{1}00$)/GaAs(111)B system are least stressed. The reduction in the stress is realized as the phase-transition stress is distributed to three equivalent directions [see Fig. 1(c)]. According to Eq. (2), ΔT is anticipated to be reduced by a factor of $(\frac{1}{3}+\frac{2}{3}\cos 60°)^2 = 0.44$, whereas we find a value of 0.6 in Fig. 4. The larger experimental value may be ascribed to the broadening of the phase transition in temperature due to the stochastic distribution of T_C for a first-order phase transition.

As evident in Fig. 4, the epitaxial stresses extend the phase coexistence primarily to low temperatures. In respect to raising T_C by a stress,[10] we find an undesirable stabilization of the β phase by the phase-transition stress. While the phase-transition stress can be manipulated through the epitaxial orientation, the thermal stress can be varied by the growth temperature. The bulk value of T_C deceases with im-

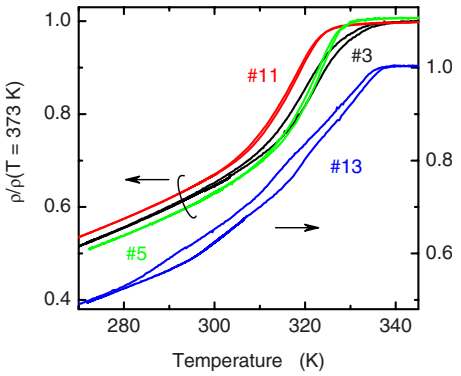

FIG. 5. (Color online) Thermal hysteresis in MnAs layers on GaAs. The resistivity ρ is normalized to the value at a temperature of $T=373$ K. The substrate orientation for the black, green, red, and blue curves are (001), No. 3, (113)A, No. 5, (111)B, No. 11, and (110), No. 13, respectively. The layers were grown by means of SPE.

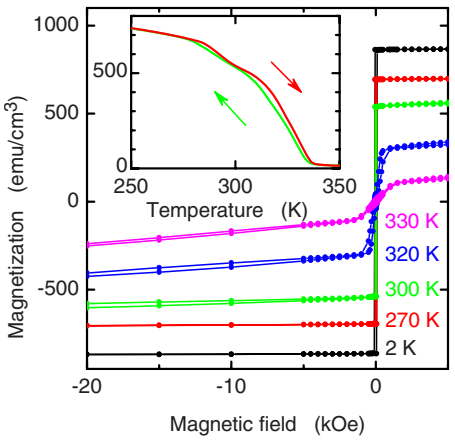

FIG. 6. (Color online) Magnetic field dependence of magnetization measured using a SQUID magnetometer at temperatures of 2, 270, 300, 320, and 330 K. The sample, No. 13, is a 140-nm-thick MnAs layer grown on GaAs(110) by means of SPE. The external magnetic field was varied between −50 and 50 kOe. The diamagnetic contribution of the GaAs substrate has been subtracted. The inset shows the temperature dependence of magnetization in the presence of an external magnetic field of 5 kOe. The red and green curves correspond to up and down temperature sweeps, respectively.

posing hydrostatic pressure.[20] The higher onset of the α phase in the C- and M-plane MnAs layers on GaAs(111)B, No. 8 and No. 11, in comparison to that in the MnAs layer on GaAs(001), No. 1, in Fig. 4 may be ascribed to the stronger tensile stress due to the higher growth temperature (see Table I).

B. Thermal hysteresis

In crossing the phase-transition temperature, a first-order phase transition does not occur immediately but is initiated when nuclei are created by surmounting a potential barrier separating the two phases. As a consequence, the phase transition is accompanied with a thermal hysteresis. In Fig. 5, we show the dependence of the hysteresis on the orientation of GaAs substrates for representative cases. In Table I, we summarize the temperature shift δT of the resistance curves between up and down temperature sweeps. The hysteresis in conventional MBE layers has been previously investigated,[7] and so we present here only the results from the layers grown by means of SPE.

The hysteresis in the layers grown on (111)- and (113)-oriented substrates is fairly small, suggesting small potential barriers for the phase transition. For (001)-oriented substrates, the MnAs layers grown by conventional MBE are of monocrystalline orientation, whereas the layers contain submicrometer-size grains of various orientations and in-plane tilts when the growth is by SPE.[12] The mixture of in-plane tilts reduces the stress, and so results in the narrow temperature interval for the phase coexistence. (The relatively large value of ΔT in No. 2 is attributed to the out-of-plane inclination of the c axis of MnAs.) Contrary to the apparent dependence of ΔT on the growth method, no clear trend is found for the thermal hysteresis between the layers grown by conventional and SPE-based procedures. The absence of generic dependence on the monocrystallinity varied by the choice of the growth method and, in particular, the smaller value of δT in No. 1 than in No. 3 are rather surprising as the most pronounced hysteresis is found for M-plane MnAs layers on GaAs(110). In the growth on GaAs(110), the participating lattices of the layer and the substrate match well.[21] The growth by means of SPE provides even a smaller orientational spread and a higher crystal quality in comparison to conventional MBE.[12] The broad hysteresis is presumed to evidence the small number of nucleation centers that trigger the phase transition as a consequence of few grain boundaries and misfit dislocations.

The phase transition and the hysteresis loop in epitaxial MnAs layers often exhibit a characteristic that defines two temperature regimes. For the bottom curve in Fig. 5, for instance, the slope of the temperature dependence changes at about 310 K, where the hysteresis gap develops a local minimum. While no anomaly has been noticed in the temperature variation in the phase fraction, the feature that emerges in the middle of the phase coexistence temperature range is present not only in resistivity but also in magnetization, as shown in the inset of Fig. 6. The dependence of magnetization on external magnetic field H applied along the magnetic easy axis (Fig. 6) reveals a change in the shape of the magnetic hysteresis. The hysteresis loop is square shaped on the low-temperature side of the phase coexistence regime. On the high-temperature side, in contrast, the magnetization reverses gradually, resembling the hard-axis behavior. In addition, the saturation magnetic field is found to increase drastically and the magnetic hysteresis expands beyond the maximum magnetic field value (± 50 kOe) of the measurements. (The data for $|H|>20$ kOe are not shown in Fig. 6.)

Ryu *et al.*[22] attributed the anomalous behavior of the magnetization to the emergence of an out-of-plane component. When temperature approaches T_C from low temperatures, disorder breaks strips of α-MnAs in the α-β stripe into short segments surrounded by β-MnAs. If the lateral dimensions of the α-MnAs islands are smaller than the layer thickness,

the shape anisotropy tilts the magnetization to the vertical direction. The mixture of the in-plane and vertical magnetization scatters conduction electrons. Therefore, an anomalous feature appears in the resistivity as well as in the magnetization even though no corresponding feature emerges in the phase fraction estimated, for instance, by x-ray diffraction (XRD).[7] The observation of the anomalous feature in the resistivity thus confirms the interpretation by Ryu *et al.*

C. Transition between the β and γ phases

The second-order structural phase transition between the β and γ phases occurs at a temperature of 398 K in bulk MnAs.[1,2] In addition to the absence of the abrupt lattice-constant change, the thermal-expansion mismatch at the temperature of the β-γ transition is only a half in comparison to that when the α-β transition occurs. The influence of the stress on the β-γ transition is hence anticipated to be small. Nonetheless, we observe considerable shifts of the β-γ transition temperature $T_{\beta\text{-}\gamma}$ in epitaxial layers, as summarized in Table I. In the inset of Fig. 4, we compare the temperature dependence of ρ in MnAs layers on GaAs(001), GaAs(113)A, and GaAs(331)B (all grown by means of SPE). Taking advantage of the negative and positive coefficients of the temperature dependence for, respectively, β- and γ-MnAs, the phase-transition temperature can be determined readily, as indicated by the arrows.

The β-γ phase-transition temperatures in the MnAs layers on GaAs(001) and GaAs(113)A are, respectively, 373 and 381 K, i.e., lower than the bulk value. In the MnAs layer on GaAs(331)B, No. 12, red curve, on the contrary, the transition temperature increases to 420 K. [The phase-transition temperature in a $(1\bar{1}00)$-oriented layer on GaAs(001) and a (0001)-oriented layer on GaAs(111)B grown by conventional MBE was, respectively, 373 and 394 K, as reported in Ref. 5, i.e., $T_{\beta\text{-}\gamma}$ is lowered.] The gradual transition between the α and β phases in the layers on (001)- and (113)A-oriented substrates occurs almost at the same temperature range (not shown), between 310 and 329 K and 313 and 329 K, respectively. For the substrate orientation of (331)B, the transition range expands to low temperatures, between 284 and 325 K (also not shown). A correlation between the phase coexistence temperature range and $T_{\beta\text{-}\gamma}$ is thus suggested.

In epitaxial layers, $T_{\beta\text{-}\gamma}$ typically decreases. As hydrostatic pressure increases $T_{\beta\text{-}\gamma}$ in bulk MnAs,[20] we attribute the lowering of $T_{\beta\text{-}\gamma}$ to the tensile stress produced by the thermal-expansion mismatch. The shift to a higher temperature when the substrate is GaAs(331)B is peculiar. The unusual shift may be related to a unique topography of the layer. Due to the step bunching during the growth of the GaAs buffer layer, $(1\bar{1}00)$- and $(11\bar{2}2)$-oriented MnAs grew on (110) terraces and sidewalls consisting of bunched steps, respectively.[12] The MnAs layer is hence zigzag shaped rather than being planar, yielding a unique distribution of stress that involves shear components.

IV. TRANSPORT PROPERTIES AT 0.3 K

A. Effect of strain on Hall resistivity

Berry *et al.*[23] reported a change in the type of majority carriers with temperature in MnAs layers on GaAs(001). The

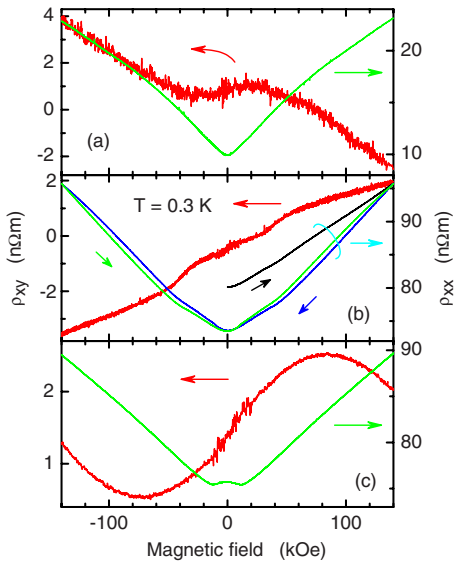

FIG. 7. (Color online) Magnetic field dependencies of transverse resistivity ρ_{xy} and longitudinal resistivity ρ_{xx} in a (a) MnAs$(1\bar{1}00)$ layer on GaAs(001), No. 1, (b) MnAs(0001) layer on GaAs(111)B, No. 8, and (c) MnAs$(1\bar{1}00)$ layer on GaAs(111)B, No. 11. The external magnetic field is applied normal to the surface. The temperature is $T=0.3$ K. The current is parallel to the $[1\bar{1}0]$ direction of the GaAs substrate. The black, blue, and green curves in (b) show ρ_{xx} in the initial and subsequent down and up magnetic field sweeps after a thermal cycle, respectively.

Hall resistivity ρ_{xy} was dominated by electrons at low temperatures, except for weak magnetic fields, where the sign of ρ_{xy} corresponded to holes. At high temperatures, however, ρ_{xy} was dominated by holes for the entire magnetic field range. In Ref. 9, we have demonstrated that the characteristics of ρ_{xy} depend also on the epitaxial orientation relationship. While the observation by Berry *et al.* was confirmed for MnAs$(1\bar{1}00)$ layers on GaAs(001), ρ_{xy} at low temperatures was dominated by holes for the entire range of magnetic field in MnAs(0001) layers on GaAs(111)B. The temperature dependence of ρ_{xy} may thus originate from the thermal strain as it induces changes in the occupation of electronlike and holelike bands at the Fermi level.

To gain more insight, we compare ρ_{xy} and the longitudinal resistivity ρ_{xx} in a MnAs$(1\bar{1}00)$ layer on GaAs(111)B [Fig. 7(c)] with those in a $(1\bar{1}00)$-oriented layer on GaAs(001) [Fig. 7(a)], and a (0001)-oriented layer on GaAs(111)B [Fig. 7(b)]. Here, the external magnetic field is applied normal to the surface. The characteristics of ρ_{xy} in the MnAs$(1\bar{1}00)$/GaAs(111)B system are in between those in the MnAs$(1\bar{1}00)$/GaAs(001) and MnAs(0001)/GaAs(111)B systems. We find a hole-dominated behavior for $|H|<70$ kOe but the slope changes to be electronlike when $|H|>80$ kOe. As we have shown in Sec. III, the layers are least stressed at room temperature in the MnAs$(1\bar{1}00)$/GaAs(111)B system. This situation does not necessarily hold at $T=0.3$ K as the thermal stress is roughly doubled in comparison to that at room temperature. The compressive stress in the MnAs(0001)/GaAs(111)B system,

for instance, is reduced at low temperatures by the increased thermal-expansion mismatch. It is unclear at present whether ρ_{xy} in Fig. 7(c) best resembles the bulk property. Comparing ρ_{xy}, the strain in the MnAs$(1\bar{1}00)$/GaAs(111)B system may be suggested to be intermediate between those in the MnAs$(1\bar{1}00)$/GaAs(001) and MnAs(0001)/GaAs(111)B systems at low temperatures.

In the MnAs layer in Fig. 7(a), the magnetization is aligned to the out-of-plane direction at about 15 kOe.[9] As this magnetic field nearly corresponds to the value at which the slope of ρ_{xy} reverses, there is a possibility that the tilting of magnetization is responsible for the low-field behavior of ρ_{xy} rather than the change in the type of dominant carriers. The Hall effect can occur in ferromagnetic materials without an external magnetic field. The Hall resistivity in the presence of the anomalous Hall effect is empirically given as[24]

$$\rho_{xy} = R_0 B + R_s M, \tag{5}$$

where R_0 and R_s are the ordinary and anomalous Hall coefficients, respectively. The induction field is given as $B = \mu_0 H + M$ with μ_0 being the permeability. The magnetoresistance in Fig. 7(c) changes from being negative to being positive at a magnetic field of 12 kOe. This feature presumably corresponds to the out-of-plane tilt of magnetization, as, in addition to the magnetic field value being similar to those found in other MnAs layers, ρ_{xy} in the weak-field region exhibits an enhancement of the measurement noise plausibly caused by the step-by-step propagation of magnetic domain walls between pinning centers. The change in the slope for ρ_{xy} in the MnAs$(1\bar{1}00)$ layer on GaAs(111)B occurs at a magnetic field that is much higher than for tilting the magnetization, and so the type of dominant carriers is unambiguously confirmed to change with magnetic field.

In order to evaluate the modification in the band occupation by strain, we have calculated the band structures using the self-consistent full-potential linearized-augmented-plane-wave method[25] for M-plane layers on GaAs(001) and C-plane layers on GaAs(111). In determining the lattice constants in the presence of the epitaxial strains, MnAs layers are assumed to be free of stress at the growth temperature. We take into account complete temperature dependence of the lattice constants[26] of both MnAs and GaAs. The strain-altered lattice constant for the C-plane MnAs layer is obtained as

$$\frac{\varepsilon_\perp}{\varepsilon_\parallel} = -2\frac{C_{13}}{C_{33}}, \tag{6}$$

where

$$\varepsilon_\parallel = \frac{a - a_r}{a_r}, \quad \varepsilon_\perp = \frac{c - c_r}{c_r}. \tag{7}$$

The suffix r indicates the lattice constants in a relaxed layer. Here, the a-axis lattice constant a obeys the thermal expansion of GaAs and the c-axis lattice constant c is determined by the consequential elastic distortion. For M-plane MnAs layers, the strain alters the hexagonal symmetry of bulk MnAs to orthorhombic symmetry. The lattice constant in this circumstance is given by

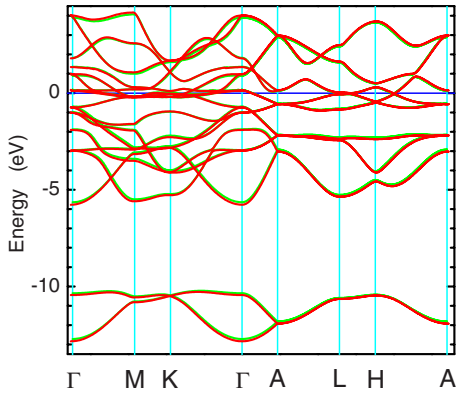

FIG. 8. (Color online) Band structure of hexagonal MnAs at temperature $T \approx 0$. The Fermi level is indicated by the blue line. For the red curves, the lattice constants are assumed to be $a=3.697$ Å and $c=5.68$ Å, which correspond to the strained C-plane MnAs. The lattice constants of bulk MnAs, $a=3.734$ Å and $c=5.67$ Å, are assumed for the green curves.

$$\varepsilon_{yy} = -\frac{C_{12}\varepsilon_{xx} + C_{13}\varepsilon_{zz}}{C_{11}}, \tag{8}$$

where ε_{xx}, ε_{yy}, and ε_{zz} are defined in manners similar to Eq. (7). The elastic constants C_{ij} (in Voigt's contracted notation) of MnAs were taken from Ref. 19. As MnAs is metal, its Fermi surface is complicated. For simplicity, we ignore the spin polarization in the following discussion since the aim of our calculation is to deduce the extent that the band structure at the Fermi level is modified by the strain.

The band structure of hexagonal MnAs along symmetry lines in the first Brillouin zone is shown in Fig. 8. The low-energy band consists of the As $4s$ states. The Fermi level is located in the p-d mixing band of As $4p$ and Mn $3d$ orbitals.[27] The difference in the band structures between the bulk, shown by green curves, and the strained MnAs that corresponds to C-plane layers, shown by red curves, is rather small. The weak dependence on the change in the lattice constants agrees with the calculation by Sanvito and Hill,[28] in which much larger lattice-constant changes were assumed to appreciably alter the band structure. Nonetheless, in regard to the properties of ρ_{xy} in epitaxial layers, the change in the effective conduction type by a strain is seen to be possible as the Fermi level, which is indicated by the blue line at zero energy in Fig. 8, is located within an energy range of dense dispersion curves. The sign of ρ_{xy} is determined as an outcome of the compensation of electronlike and holelike contributions. Although we ignored the spin polarization, we do not expect it to alter this conclusion. The calculation by Li *et al.*,[29] in which the spin polarization was fully taken into account, reveals a band structure similar, in principle, to that in Fig. 8.

For the M-plane-oriented MnAs, the lattice constants are estimated to be $a=3.697$ Å, $b=3.759$ Å, and $c=5.781$ Å. The thermal distortion to orthorhombic symmetry (1.7%) is even larger in magnitude than the phase-transition distortion at T_C. The band structure of the M-plane-oriented MnAs shows again a fairly small modification resulting from the

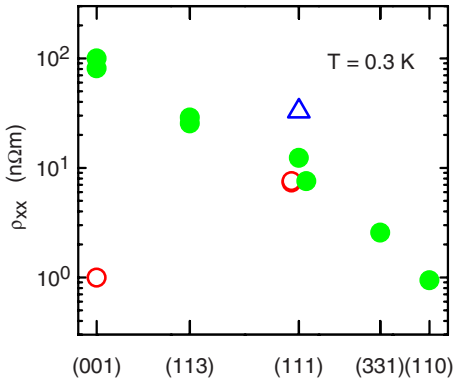

FIG. 9. (Color online) Residual resistivity (longitudinal resistivity ρ_{xx} at a temperature of $T=0.3$ K) in MnAs layers grown on GaAs substrates having (001), (113)A, (111)B, (331)B, and (110) orientations. The filled and open circles correspond to the layers grown by conventional MBE and by means of SPE, respectively. The layer was grown by a conventional growth at a substrate temperature of 220 °C, No. 10, for the triangle.

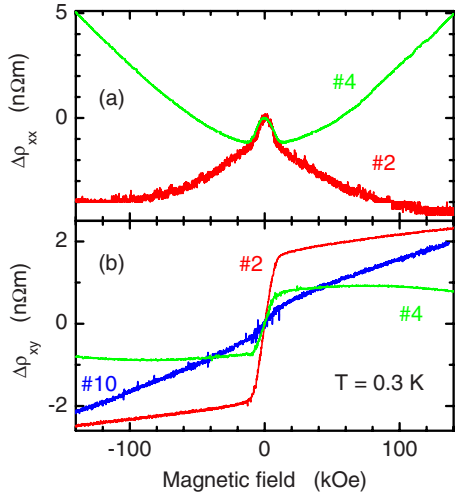

FIG. 10. (Color online) Dependence of $\Delta\rho=\rho(H)-\rho(H=0)$ on external magnetic field H applied normal to the surface for (a) longitudinal resistivity ρ_{xx} and (b) transverse resistivity ρ_{xy} at temperature $T=0.3$ K. The MnAs layers were grown on GaAs(001), No. 2 (red curve), and GaAs(113)A, No. 4 (green curve), by means of SPE. The blue curve in (b) was obtained from a MnAs layer on GaAs(111)B, No. 10, in which the surface orientation is a mixture of M plane (83%) and C plane (17%). The zero-field resistivity was 809 and 254 nΩ m for No. 2 and No. 4, respectively.

change in the lattice constants in comparison to that of bulk MnAs (not shown). However, as demonstrated by Motizuki *et al.*,[30] lowering the symmetry from hexagonal to orthorhombic introduces splitting of the degenerate energy levels in the folded dispersion curves of the original hexagonal structure. The strain thus alters the band structure more efficiently in M-plane layers than in C-plane layers, at least in the way to influence ρ_{xy}. The temperature dependence of ρ_{xy} driven by the thermal strain is anticipated to be stronger in M-plane layers than in C-plane layers.

B. Dependence on residual resistivity

As one may speculate from the red and black curves in Fig. 4, Nos. 4 and 8, the residual resistivity depends on the substrate orientation and growth method. In Fig. 9, we compare the values of ρ_{xx} at $T=0.3$ K in MnAs layers grown by means of SPE (filled circles) and conventional MBE (open symbols). The scattering from the structural domain boundaries and magnetic domain walls is demonstrated to be capable of spreading the residual resistivity over, at least, 2 orders of magnitude. The most dramatic case is found for (001)-oriented substrates. The MnAs layers grown on GaAs(001) are of monocrystalline orientation with the conventional MBE, whereas the layers grown using SPE is polycrystalline.[12] Therefore, ρ_{xx} is much higher for the SPE-based growth than for the conventional growth. The relatively large value of ρ_{xx} when the substrate is GaAs(113)A is consistent with the speculation based on XRD in Ref. 12 that the layers consist of microcrystallites.

For GaAs(111)B substrates, the residual resistivities in C-plane layers grown by conventional MBE and in M-plane layers grown by means of SPE are unexpectedly very similar despite the inherent structural domains in the latter. The C-plane of MnAs is the magnetic easy plane, and so the magnetization can be, in principle, oriented in any in-plane directions if a magnetocrystalline anisotropy was not introduced by the substrate. The scattering from such magnetic randomness in the C-plane layers is suggested to be as strong as the scattering from the structural domains in the M-plane layers. We point out that a large number of extremely strong pinning centers of domain walls are present in the layers on GaAs(111)B, as we will show in Sec. IV C. The magnetic disorder is thus stronger than in ordinary ferromagnetic layers. The triangle in Fig. 9 indicates the value in a MnAs layer prepared by a conventional growth on GaAs(111)B, No. 10. Because of the low growth temperature of 220 °C, the layer is composed of both an M-plane component (83%) and a C-plane component (17%). The addition of the normal-to-surface c-axis orientation is seen to be more efficient to increase ρ_{xx} than the randomness in the in-plane c-axis orientation.

The resistance of materials containing magnetic moments generally decreases in the presence of an external magnetic field. In a high magnetic field, the magnetic moments are aligned in the direction of the field. The scattering of conduction carriers from random orientations of the magnetic moments is hence suppressed. In Fig. 7, however, the magnetoresistance is positive. We attribute the positive magnetoresistance to small values of ρ_{xx} in these layers. When the transverse conductivity σ_{xy} is much larger than the longitudinal conductivity σ_{xx}, matrix inversion of conductivity tensor yields $\rho_{xx}=\sigma_{xx}/(\sigma_{xx}^2+\sigma_{xy}^2)\approx\sigma_{xx}/\sigma_{xy}^2$. Thus, a positive magnetoconductance arising from the suppression of magnetic scattering can result in a positive magnetoresistance. This interpretation is supported in Fig. 10(a), in which the magnetoresistance is negative due to the large residual resistivity. We note however that σ_{xx} calculated using ρ_{xx} and ρ_{xy} in Fig. 7 does not exhibit positive magnetoconductance. This implies that the relation between the experimentally measured resistance and the resistivity or conductivity tensor that

adequately describes the microscopic mechanism of the scattering events is rather complicated. In this respect, it is interesting to notice that, despite the factor of ≈3 difference in the residual resistivity, the $\Delta\rho_{xx}$ curves in Fig. 10(a) are nearly identical in the low-field regime where the magnetization is reoriented. This might imply that ρ_{xx} is the fundamental quantity that provides a universal amplitude of the magnetoresistance associated with the magnetization reorientation.

In MnAs layers having large values of ρ_{xx}, ρ_{xy} is dominated by the anomalous Hall effect,[31] as shown in Fig. 10(b). Several different mechanisms have been proposed to calculate R_s in Eq. (5). All of them, the skew scattering and side-jump mechanisms as well as Berry phase contribution, depend on the spin-orbit interaction.[32,33] The agreement between the experiment and theory has not been yet satisfactory. We would like to make a remark here concerning the dependence of R_s on ρ_{xx}. In Fig. 10(b), we also include ρ_{xy} in No. 10. Although the residual resistivity of No. 10 is similar to that of No. 4, the anomalous Hall effect is significantly smaller in No. 10 than in No. 4. The magnitude of anomalous Hall effect is thus not a unique function of the residual resistivity unless the polycrystalline nature of these layers played a role for the seeming independence on the residual resistivity.

C. Extremely strong domain-wall pinning

As we have reported in Ref. 34, the magnetoresistance in *C*-plane MnAs layers on GaAs(111)B evidences the existence of a magnetization component that does not saturate even when the in-plane external magnetic field is as strong as 140 kOe. An example obtained from No. 8 is shown in Figs. 11(b) and 11(c). The magnetic hysteresis extends to the entire range of the magnetic field of the measurements. In addition, the resistance decreases dramatically after application of the field in comparison to that in a demagnetized state generated by a thermal cycle. The magnetization reversal takes place via the domain-wall movement across the layer. The hysteresis thus implies extremely strong pinning of magnetic domain walls in the layer. The unsaturated magnetic hysteresis is present irrespective of the direction of the magnetic field as shown in Fig. 7(b), in which the field is applied normal to the layer. The hysteretic behavior is less pronounced here in comparison to the case of the in-plane magnetic field, plausibly because the direction of the field is perpendicular to the magnetic easy axis. Nonetheless, the pinning centers are seen to obstruct not only the flipping of magnetization along the magnetic easy axis but also the gradual tilting to the out-of-plane hard-axis direction. The strong domain-wall pinning, however, does not seem to affect ρ_{xy}. The indifference is presumably related to the fact that anisotropic magnetoresistance effect in ρ_{xy} vanishes when the angle between the magnetization and current is 0° or 90°.[9,24] The pinning hinders the flipping of magnetization components but does not tilt them to be away from the magnetic easy axis.

A crucial characteristic that will help identifying the mechanism of the extremely strong domain-wall pinning is

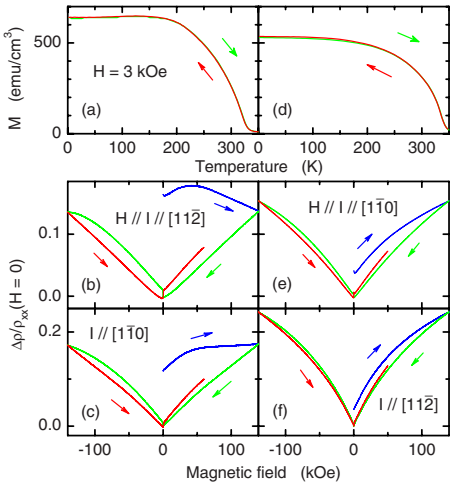

FIG. 11. (Color online) Temperature dependence of magnetization M and magnetoresistance $\Delta\rho/\rho_{xx}(H=0)$ with $\Delta\rho=\rho_{xx}(H)-\rho_{xx}(H=0)$ at a temperature of 0.3 K. The left- and right-hand-side columns correspond to two different *C*-plane MnAs layers on GaAs(111)B, respectively, No. 8 and No. 9, grown under practically identical conditions. The layers exhibited almost the same zero-field resistivity of ≈74 nΩ m. The magnetization, (a) and (d), was measured in the presence of an in-plane external magnetic field of $H=3$ kOe. The samples were cooled in the absence of the external field prior to the up and down temperature sweeps. The contribution of the GaAs substrates has been subtracted. In (b), (c), (e), and (f), the directions of H and the current I with respect to the substrate orientation are indicated. The blue curves show the initial trace after a thermal cycle. The green and red curves were obtained in the subsequent down and up field sweeps, respectively.

seen in Fig. 11(a). The magnetization deceases below about 100 K with decreasing temperature, reminding us of antiferromagnetic or spin-glass system. Here, the sample was cooled in the absence of an external magnetic field. The magnetization was measured in the following up and down temperature sweeps in the presence of an in-plane external magnetic field of 3 kOe. As the difference between the zero-field-cooled and field-cooled curves is small, the anomalous magnetization component is suggested to be rather antiferromagneticlike than spin-glass-like.

We show in Figs. 11(e) and 11(f) the transport properties in a different layer, No. 9, grown under practically identical conditions together with the temperature dependence of magnetization plotted in Fig. 11(d). The residual resistivities in the two layers No. 8 and No. 9 were identical within the experimental accuracy. All of the anomalous characteristics, (i) the unsaturated hysteretic magnetoresistance, (ii) the large decrease in the resistance after magnetizing the layer, and (iii) the low-temperature decrease in the magnetization, are seen to be smaller in No. 9 than in No. 8. This demonstrates a correlation between the anomalous magnetization component and the extremely strong domain-wall pinning. The nonferromagnetically ordered magnetic moments corresponding to the low-temperature decrease in the magnetization are suggested to act as the strong pinning centers. Despite the fairly small fraction of the anomalous magnetization component, its influence on the magnetotransport properties is remarkably large. It may be noteworthy

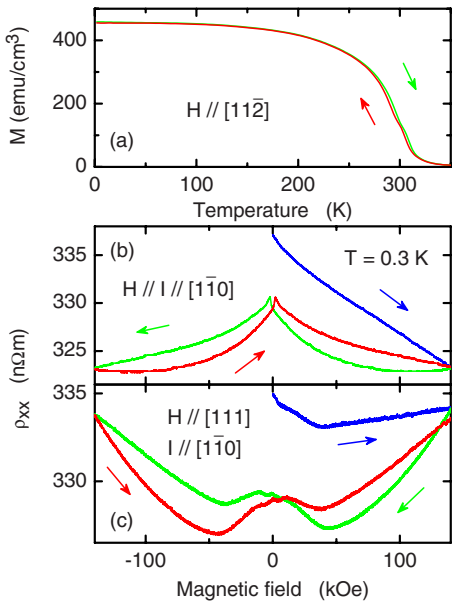

FIG. 12. (Color online) (a) Temperature dependence of magnetization M and (b) and (c) magnetic field dependence of longitudinal resistivity ρ_{xx} at temperature $T=0.3$ K. The MnAs layer, No. 10, was grown on GaAs(111)B by conventional MBE at a growth temperature of 220 °C. The magnetization was measured in the presence of an in-plane external magnetic field of $H=5$ kOe applied along the $[11\bar{2}]$ direction of the substrate. A cooling of the sample at $H=0$ was followed by the up and down temperature sweeps. The blue, green, and red curves in (b) and (c) correspond to the initial sweep after a thermal cycle and subsequent down and up field sweeps, respectively.

that the hysteresis is larger when $H\|I$ than when $H\perp I$ in both of the layers.

While the origin of the nonferromagnetically ordered, i.e., antiferromagneticlike or spin-glass-like, magnetic moments is presently unclear, we have found that the phenomenon of the extremely strong domain-wall pinning takes place also in a layer having mixed M- and C-plane orientations, No. 10, as shown in Fig. 12. The external magnetic field is applied in an in-plane direction in Fig. 12(b) and normal to the surface in Fig. 12(c). (The magnitude of the anomalous features in this layer was comparable between the situations where the current was parallel and perpendicular to the in-plane field.) The magnetic coupling between the two structural components is suggested to give rise to the strong domain-wall pinning. However, the magnetization plotted in Fig. 12(a) does not decrease at low temperatures. We have neither found evidence for a mixture of the M-plane orientation in No. 8. It remains to be clarified whether the mechanisms for the strong domain-wall pinning in No. 8 and No. 10 are identical. We emphasize, nevertheless, that the anomalous behavior has been observed so far only in layers grown on GaAs(111)B substrates. If antiferromagneticlike magnetic moments do exit in α-MnAs layers on GaAs(111)B, the compressive strain may play a role as the Mn-Mn coupling can change from being ferromagnetic to being antiferromagnetic when the interatomic distance is varied.[35]

V. SUMMARY

We have investigated the transport properties in the MnAs layers grown on various substrate orientations by means of conventional and SPE-based MBE. The stress in these layers ranges widely due to the variation in the c-axis orientation, as manifested by the temperature interval for the coexistence of the α and β phases. The negative temperature coefficient of the resistivity of β-MnAs is robust, indicating the existence of a generic mechanism for the unusual temperature dependence, which may be an antiferromagnetic order. The polarity of the Hall coefficient changes remarkably by the strain associated with the epitaxial orientation. Our band-structure calculations indicate this to be a consequence of subtle changes in the occupation of dense dispersion curves. The residual resistivity in the layers can be varied over, at least, 2 orders of magnitude by controlling the scattering from the structural and magnetic domains. This can be exploited, for instance, to investigate anomalous Hall effect. We have provided evidence for the dependence on the residual resistivity of the relative amplitudes of the ordinary and anomalous Hall effects as well as the relation between the longitudinal and transverse conductivities or resistivities. However, no clear trend has been identified so far, which might suggest that the microscopic mechanism of the residual scattering plays a role. We have also shown that extremely strong domain-wall pinning emerges when the layer is composed of both M- and C-plane surface orientations. The substrate orientation being (111)B appears to be crucial for this phenomenon.

[1] C. Guillaud, J. Phys. Radium **12**, 223 (1951).
[2] R. H. Wilson and J. S. Kasper, Acta Crystallogr. **17**, 95 (1964).
[3] M. K. Niranjan, B. R. Sahu, and L. Kleinman, Phys. Rev. B **70**, 180406(R) (2004).
[4] H. Yamaguchi, A. K. Das, A. Ney, T. Hesjedal, C. Pampuch, D. M. Schaadt, and R. Koch, Europhys. Lett. **72**, 479 (2005).
[5] Y. Takagaki, L. Däweritz, and K. H. Ploog, Phys. Rev. B **75**, 035213 (2007).
[6] M. Tanaka, Semicond. Sci. Technol. **17**, 327 (2002).
[7] L. Däweritz, Rep. Prog. Phys. **69**, 2581 (2006).
[8] K.-J. Friedland, M. Kästner, and L. Däweritz, Phys. Rev. B **67**, 113301 (2003).
[9] Y. Takagaki and K.-J. Friedland, J. Appl. Phys. **101**, 113916 (2007).
[10] V. Garcia, Y. Sidis, M. Marangolo, F. Vidal, M. Eddrief, P. Bourges, F. Maccherozzi, F. Ott, G. Panaccione, and V. H. Etgens, Phys. Rev. Lett. **99**, 117205 (2007); N. Mattoso, M. Eddrief, J. Varalda, A. Ouerghi, D. Demaille, V. H. Etgens, and Y. Garreau, Phys. Rev. B **70**, 115324 (2004).
[11] Y. Takagaki, C. Herrmann, B. Jenichen, J. Herfort, and O.

Brandt, Appl. Phys. Lett. **92**, 101918 (2008); **92**, 179901(E) (2008).
[12] Y. Takagaki, C. Herrmann, B. Jenichen, and O. Brandt, Phys. Rev. B **78**, 064115 (2008).
[13] V. M. Kaganer, B. Jenichen, F. Schippan, W. Braun, L. Däweritz, and K. H. Ploog, Phys. Rev. Lett. **85**, 341 (2000); Phys. Rev. B **66**, 045305 (2002).
[14] V. H. Etgens, M. Eddrief, D. Demaille, Y. L. Zheng, and A. Ouerghi, J. Cryst. Growth **240**, 64 (2002).
[15] D. K. Satapathy, V. M. Kaganer, B. Jenichen, W. Braun, L. Däweritz, and K. H. Ploog, Phys. Rev. B **72**, 155303 (2005).
[16] The temperature coefficient for β-MnAs was positive in No. 11, as one can see in Fig. 4.
[17] C. Timm, M. E. Raikh, and F. von Oppen, Phys. Rev. Lett. **94**, 036602 (2005); G. Zaránd, C. P. Moca, and B. Jankó, *ibid.* **94**, 247202 (2005); V. Novák, K. Olejník, J. Wunderlich, M. Cukr, K. Výborný, A. W. Rushforth, K. W. Edmonds, R. P. Campion, B. L. Gallagher, J. Sinova, and T. Jungwirth, *ibid.* **101**, 077201 (2008).
[18] Y. Takagaki, E. Wiebicke, L. Däweritz, and K. H. Ploog, Appl. Phys. Lett. **85**, 1505 (2004).
[19] M. Dörfler and K. Bärner, Phys. Status Solidi A **17**, 141 (1973).
[20] N. Menyuk, J. A. Kafalas, K. Dwight, and J. B. Goodenough, Phys. Rev. **177**, 942 (1969).
[21] D. Kolovos-Vellianitis, C. Herrmann, L. Däweritz, and K. H. Ploog, Appl. Phys. Lett. **87**, 092505 (2005).
[22] K. Ryu, J. Kim, Y. Lee, H. Akinaga, T. Manago, R. Viswan, and S. Shin, Appl. Phys. Lett. **92**, 082503 (2008).
[23] J. J. Berry, S. J. Potashnik, S. H. Chun, K. C. Ku, P. Schiffer, and N. Samarth, Phys. Rev. B **64**, 052408 (2001).
[24] T. R. McGuire and R. I. Potter, IEEE Trans. Magn. **11**, 1018 (1975).
[25] P. Blaha, K. Schwarz, and P. H. Dederichs, Phys. Rev. B **38**, 9368 (1988).
[26] T. Suzuki and H. Ido, J. Phys. Soc. Jpn. **51**, 3149 (1982).
[27] K. Motizuki and K. Katoh, J. Phys. Soc. Jpn. **53**, 735 (1984).
[28] S. Sanvito and N. A. Hill, Phys. Rev. B **62**, 15553 (2000).
[29] M. Li, T. Ariizumi, K. Koyanagi, and S. Suzuki, Jpn. J. Appl. Phys., Part 1 **46**, 3455 (2007).
[30] K. Motizuki, K. Katoh, and A. Yanase, J. Phys. C **19**, 495 (1986).
[31] M. Lee, Y. Onose, Y. Tokura, and N. P. Ong, Phys. Rev. B **75**, 172403 (2007).
[32] N. Nagaosa, J. Phys. Soc. Jpn. **75**, 042001 (2006).
[33] P. Wölfle and K. A. Muttalib, Ann. Phys. **15**, 508 (2006).
[34] Y. Takagaki, J. Herfort, and K.-J. Friedland, Phys. Rev. B **76**, 184409 (2007).
[35] L. M. Sandratskii, R. Singer, and E. Şaşioğlu, Phys. Rev. B **76**, 184406 (2007).